





Observation of soft Leggett mode in superconducting $\text{CaKFe}_4\text{As}_4$

S. Z. Zhao ¹, Hai-Ying Song ¹, L. L. Hu,² T. Xie,^{3,4,*} C. Liu,^{3,4} H. Q. Luo,^{3,5} Cong-Ying Jiang,¹ Xiu Zhang,¹ X. C. Nie,¹ Jian-Qiao Meng ⁶, Yu-Xia Duan,⁶ Shi-Bing Liu,^{1,*} Hong-Yi Xie,^{2,*} and H. Y. Liu ^{1,2,*}

¹Strong-field and Ultrafast Photonics Lab, Beijing Engineering Research Center of Laser Technology, Institute of Laser Engineering, Beijing University of Technology, Beijing 100124, People's Republic of China

²Beijing Academy of Quantum Information Sciences, Beijing 100193, People's Republic of China

³Beijing National Laboratory for Condensed Matter Physics, Institute of Physics, Chinese Academy of Sciences, Beijing 100190, People's Republic of China

⁴School of Physical Sciences, University of Chinese Academy of Sciences, Beijing 100190, People's Republic of China

⁵Songshan Lake Materials Laboratory, Dongguan, Guangdong 523808, People's Republic of China

⁶School of Physics and Electronics, Central South University, Changsha, Hunan 410083, People's Republic of China



(Received 11 July 2019; revised 18 May 2020; accepted 7 October 2020; published 21 October 2020)

We study the ultrafast dynamics of the multiband iron-based superconductor $\text{CaKFe}_4\text{As}_4$ via time-resolved optical reflectivity. We observe a long-lived 5-GHz oscillation of the reflection changes within the superconducting regime. We assign this low-frequency oscillation to a soft Leggett mode associated with the collective fluctuation of multiple phase differences between Cooper pair condensates. Our observation evidences the presence of the time-reversal-symmetry breaking state in superconducting $\text{CaKFe}_4\text{As}_4$.

DOI: [10.1103/PhysRevB.102.144519](https://doi.org/10.1103/PhysRevB.102.144519)

I. INTRODUCTION

The Leggett mode in multiband superconductors has been of great interest since it was predicted half a century ago [1]. For multiple Josephson-coupled condensates on unconnected sheets of the Fermi surface, the Leggett mode corresponds to collective excitations of the interband phase differences, which is analogous to the plasma mode in multiterminal Josephson junctions. The Leggett mode is charge neutral and gapped, and its zero-point energy strongly depends on the pairing symmetry [2–4] as well as the number of the superconducting (SC) gaps and the interplay of the intra- and interband Josephson couplings [5–14]. In the two-band superconductors with conventional s -wave pairing, the Leggett mode is determined by the interband coupling and usually heavy and short-lived. As observed in MgB_2 with various spectroscopies [15–19], the mode lies between the two SC gaps and, therefore, rapidly decays into the quasiparticle (QP) continuum associated with the band of the smaller gap. The observation is well consistent with the theoretical calculation [5–7].

The iron-based superconductors often exhibit multiple SC gaps with unconventional s -wave symmetry attributed to strong interband repulsion [20,21]. Theoretical analysis of a two-band model has demonstrated that the Leggett mode is absent in the SC regime dominated by interband coupling, which is contrary to the intraband-dominant situation as in MgB_2 [13]. In systems with three or more bands, the properties of Leggett mode are more intriguing. There exist multiple

branches of Leggett mode that can be classified into dynamical classes [9]. Moreover, it has been proposed that the lowest branch can be dramatically softened and become massless, which is a signature of the time-reversal-symmetry breaking state directed by interband phase frustration [12–14]. This soft Leggett mode ought to be long-lived since it is far below the QP continuum. Nevertheless, there is still lack of experimental observation of a soft Leggett mode in various iron pnictides.

The recently discovered $\text{CaKFe}_4\text{As}_4$ compound [22] seems to be an ideal platform to investigate the Leggett mode in multiband pnictides. Undoped $\text{CaKFe}_4\text{As}_4$ has a relatively high transition temperature $T_c \approx 35$ K [23–25]. Angle-resolved photoemission spectroscopy (ARPES) measurement has resolved three SC gaps on the hole pockets (the Γ point) and one gap on the electron pocket (the M point) [23]. Inelastic neutron scattering study has evidenced that the superconductivity is dominated by the unconventional s -wave pairing due to strong interpocket repulsion enhanced by spin fluctuations [26]. A numerical simulation combining *ab initio* and tight-binding methods has suggested up to ten SC gaps with competing pair couplings [27]. Structurally, its Ca and K layers are alternatively ordered without site inversions, so that the substitution disorder is suppressed [28]. In addition, the electronic nematicity, that is a common feature of many iron-based compounds, seems to be absent in $\text{CaKFe}_4\text{As}_4$ [29], and, therefore, the superconductivity suffers less competing or coexisting orders.

The time-resolved optical spectroscopy based on femtosecond lasers has been proven to be a powerful tool to observe the Leggett mode [19]. The electromagnetic field couples to the mode via the nonlinear Raman processes [30–32]. The photoexcited interband phase imbalance is analogous to the ac Josephson effect: a vector potential $a(t)$ simultaneously

*Corresponding authors: sbliu@bjut.edu.cn; xiehy@baqis.ac.cn; li-uh@baqis.ac.cn

creates an effective voltage $\propto |a(t)|^2$ on each condensate, so that the corresponding phase evolves in time $\propto \int_0^t dt' |a(t')|^2$, where the prefactor is proportional to the inverse of the band effective mass [32]. This phase imbalance is proportional to the pump fluence and significant between structurally distinct bands, e.g., the electron- and holelike bands. In correlated electron systems, out-of-equilibrium excitations, such as quasiparticles, supragap incoherent phonons, and Raman-active collective modes, are first excited by a pump pulse and their subsequent temporal evolution is detected by a second probe pulse. The reflection (or transmission) change of the probe $\Delta R/R$ (or $\Delta T/T$) is inferred to be the combination of the photoexcited QP density [33] and the collective-mode amplitudes [34–39]. Photoexcited QPs lose energy through interactions with various degrees of freedom, leading to multiple characterized relaxations in the ultrafast time domain [40–46].

In this Letter, we report the observation of a soft Leggett mode in $\text{CaKFe}_4\text{As}_4$ via time-resolved optical reflectivity. In the picosecond regime, we observe three temperature- and fluence-independent relaxation times, that are due to the normal-state QP dynamics and irrelevant to the superconductivity. In the subnanosecond regime and within the SC phase, we observe the coexistence of two types of dynamics: (i) the SC QP recovery governed by the boson-bottleneck effect, and (ii) a long-lived oscillation of frequency 5 GHz, that we identify as a soft Leggett mode. This oscillation mode contrasts the coherent phonon modes in the Ca-122 materials, which persist even above T_c and possess strongly temperature-dependent frequencies and phases [37]. We do not observe the signature associated with the spin density wave [44–46].

II. METHOD

Highly homogeneous single crystals of $\text{CaKFe}_4\text{As}_4$ were grown by the self-flux method [26]. In the ultrafast time-resolved optical reflectivity measurements, the infrared pulses of 35 fs were produced by a Ti:Sapphire amplifier working at a repetition rate of 1 kHz with a central wavelength at 800 nm. The pump and probe beams were focused onto the sample surface almost collinearly, with spot sizes of about 0.4 and 0.2 mm in diameter, respectively, ensuring that all probe signals emitted from the photoexcited volume. The probe signal was collected by a Si-based detector and a lock-in amplifier in order to record the transient reflectivity changes $\Delta R/R$. The sample crystal was glued on a copper base mounted on a cryostat, allowing a temperature control from 5 to 300 K. The probe fluence was kept a constant of $0.6 \mu\text{J}/\text{cm}^2$, minimizing the probe perturbation compared to the pump ($\gg 6 \mu\text{J}/\text{cm}^2$).

III. RESULTS AND DISCUSSION

Figure 1 shows the transient reflectivity changes $\Delta R/R$ at various temperatures from 5 to 50 K for a fixed pump fluence $F = 120 \mu\text{J}/\text{cm}^2$. It manifests that every $\Delta R/R$ curve is composed of multiple relaxation components. The picosecond ($t < 50$ ps) signals are nearly temperature-independent in the normal phase, but significantly enhanced as temperature decreases in the SC phase. This enhancement reflects the intrinsic relationship between the initial population of the

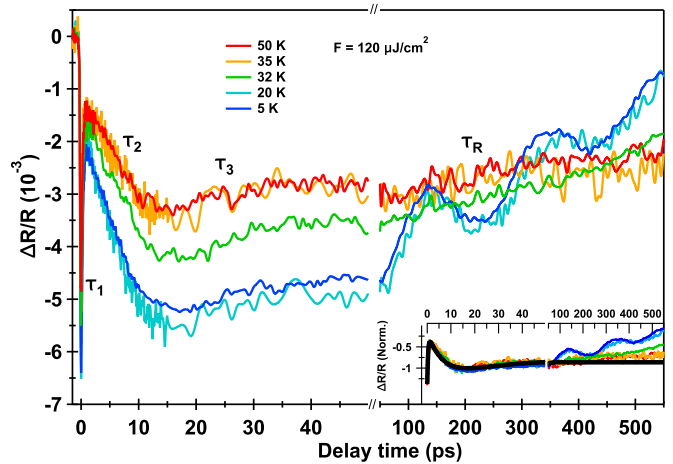


FIG. 1. Transient reflectivity changes $\Delta R/R$ as a function of temperature for a fixed pump fluence $F = 120 \mu\text{J}/\text{cm}^2$. The results in the picosecond regime $t < 50$ ps and in the subnanosecond regime $t > 50$ ps are presented in different time scales. The inset shows normalized $\Delta R/R$ curves. The black curve represents a triexponential fit of the picosecond signals yielding three characteristic times $\tau_{1,2,3}$. The subnanosecond result is further analyzed in Figs. 2–4.

photoexcited QPs and the SC gaps, as we later discuss in Fig. 2. The subnanosecond ($t > 50$ ps) signals show remarkable oscillations within the SC phase, that we later investigate in Figs. 3 and 4. In the inset of Fig. 1, we show the normalized signals. In picosecond regime, using a tri-exponential fit we extract three temperature-independent relaxation times $\tau_1 = 0.4 \pm 0.1$ ps, $\tau_2 = 8.0 \pm 1.3$ ps, and $\tau_3 = 12.8 \pm 3.2$ ps. These short-time scales are attributed to the supragap normal-state QP relaxation, which depends on the band structure of $\text{CaKFe}_4\text{As}_4$ compound. To clarify the origin of these relax-

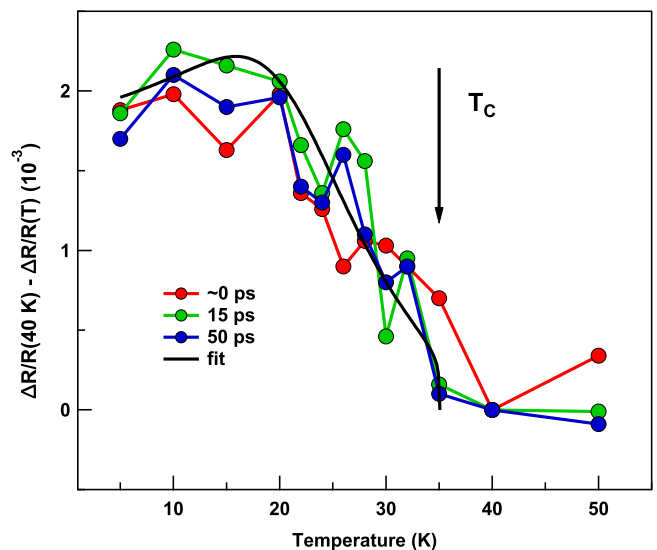


FIG. 2. Superconductivity-enhanced amplitudes $|\Delta R/R(T) - \Delta R/R(40 \text{ K})|$ as a function of temperature at ~ 0 (the sharp dip), 15, and 50 ps extracted from Fig. 1. The black curve represents the fit of the result at 15 ps based on Eq. (3), yielding the zero-temperature gap $\Delta(0) = 10 \pm 1$ meV.

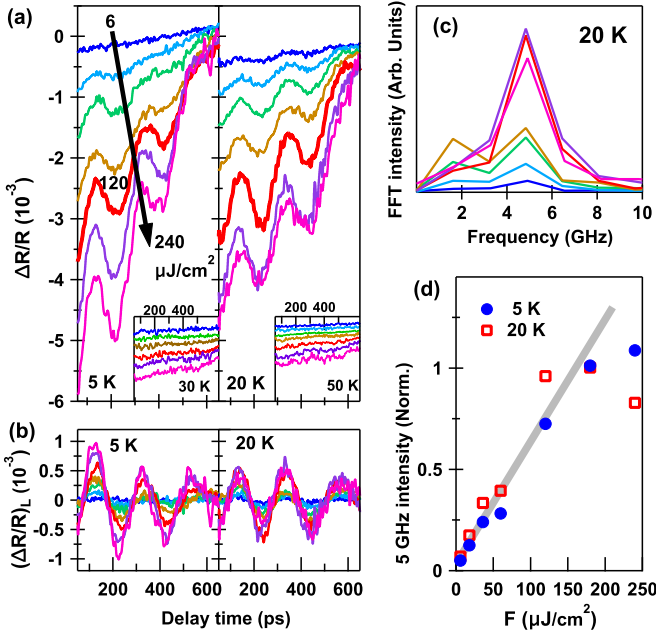


FIG. 3. Characteristics of coherent oscillations as a function of pump fluence. (a) Subnanosecond $\Delta R/R$ signals for various fluences from 6 to 240 $\mu\text{J}/\text{cm}^2$ at $T = 5, 20, 30,$ and 50 K. (b) Coherent oscillations $(\Delta R/R)_L$ extracted from the result in (a) by subtracting the exponential decay of each curve according to Eq. (3). (c) FFT curves of the result in (b). (d) FFT peak intensity versus the pump fluence. The gray line is used to guide the eye for a linear relation.

ation times, further analysis based on time-resolved ARPES measurement and *ab initio* calculation is essentially required, which is out of the scope of this work.

We focus on investigating the subnanosecond signals that reveal the temporal dynamics of the excitations dominated by the superconductivity. We describe the transient reflectivity changes by the phenomenological formula

$$\Delta R/R = (\Delta R/R)_{\text{bn}} + (\Delta R/R)_L + \mathcal{C}, \quad (1)$$

where $(\Delta R/R)_{\text{bn}}$ [Eq. (2)] and $(\Delta R/R)_L$ [Eq. (5)] represent the contributions from the QP boson-bottleneck effect and the Leggett mode, respectively, and \mathcal{C} describes an ultraslow process towards global equilibrium such as the thermal diffusion, which is out of the measurement domain.

It has been well understood that in a superconductor the long-time relaxation dynamics of photoexcited quasiparticles below T_c is governed by the boson-bottleneck effect [47–49]. After an initial pulse stimulation, the quasiparticles relax and temporarily accumulate above the SC gaps. The subsequent processes of intra- or interband QP combination and regeneration are dominated by emission and absorption of a certain type of bosons with energies higher than the sum of the two relevant gaps. These processes are accompanied by the decay of the boson population governed either by anharmonic decay to low-frequency bosons or escape to the boson reservoir [44]. Via the Rothwarf-Taylor model [50], we obtain the corresponding reflectivity changes

$$(\Delta R/R)_{\text{bn}} = -\mathcal{A}e^{-t/\tau_{\text{R}}}, \quad (2)$$

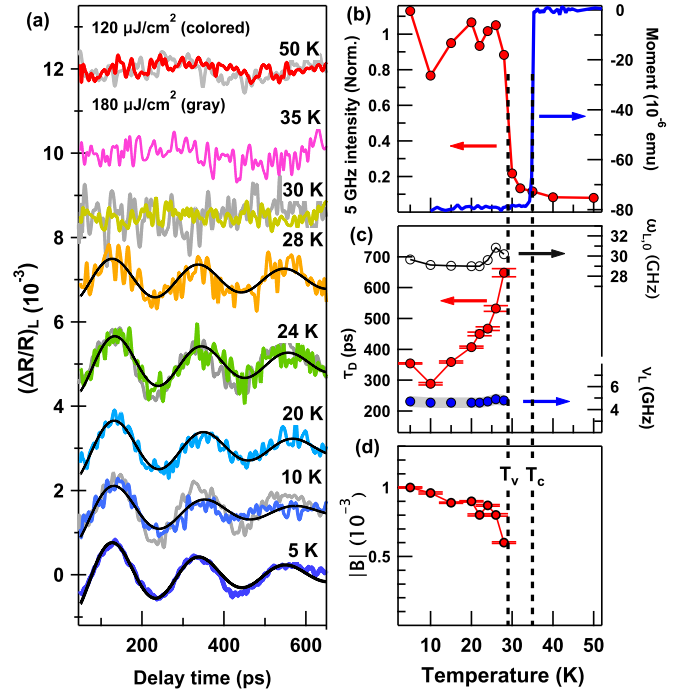


FIG. 4. Characteristics of coherent oscillations as a function of temperature. (a) $(\Delta R/R)_L$ signals from 5 to 50 K for fluences 120 and 180 $\mu\text{J}/\text{cm}^2$. The black curves depict the fits of the lower fluence signals by using Eq. (5). (b) Normalized FFT amplitude of the lower fluence signals (the red curve). The oscillation mode becomes invisible for $T > T_v \approx 29$ K. We show the SC transition $T_c \approx 35$ K signals (the blue curve) obtained by a magnetic measurement (Zero-field cooled and $H = 10$ Oe). (c) and (d) Frequencies ν_L , $\omega_{L,0}$ and damping time τ_D and initial amplitude \mathcal{B} as functions of temperature, respectively, extracted from (a).

where \mathcal{A} is proportional to the initially excited QP density, and τ_{R} is the pair recovery time that is inversely proportional to the typical gap and diverges nearby T_c .

As shown Fig. 2, we extract the temperature dependence of the amplitudes $\mathcal{A} = |\Delta R/R(T) - \Delta R/R(40 \text{ K})|$ in Eq. (2) from the picosecond signals in Fig. 1. We find that the superconductivity-enhanced amplitudes \mathcal{A} are almost time-independent within 50 ps. Assuming identical SC gaps $\Delta(T)$, we exploit the expression [51]

$$\mathcal{A}(T) \propto \frac{\epsilon_I / [\Delta(T) + k_B T / 2]}{1 + \beta \sqrt{\frac{2k_B T}{\pi \Delta(T)}} \exp[-\Delta(T) / k_B T]}, \quad (3)$$

where ϵ_I and β are the pump excitation intensity per unit cell and the boson-related parameter, respectively. Using a Bardeen-Cooper-Schrieffer-like gap form $\Delta(T) = \Delta(0)\sqrt{1 - T/T_c}$, we estimate $\Delta(0) = 10 \pm 1$ meV, which coincides with the average value of the four SC gaps of $\text{CaKFe}_4\text{As}_4$ resolved by ARPES measurement [23].

We turn to analyzing the oscillatory components of the subnanosecond signals. Regardless of the microscopic detail, we introduce the damped oscillator model to describe the temporal dynamics of a Leggett mode associated with multiple

TABLE I. Zero-temperature characteristics of the coherent oscillations [Eqs. (5)] obtained from the results in Fig. 4.

$\Delta(0)$	$\omega_{L,0}(0)$	$\tau_D^{-1}(0)$	$Q(0)$	α
10 meV	31 GHz	4 GHz	4	2×10^{-3}

equiamplitude gaps,

$$\frac{1}{\omega_{L,0}^2} \frac{d^2\phi}{dt^2} + \frac{1}{\omega_{L,0}Q} \frac{d\phi}{dt} + \phi = 0. \quad (4)$$

Here ϕ is an effective phase variable, which is generally a linear combination of the interband phase fluctuations. The zero-point energy $\hbar\omega_{L,0}(T) \equiv \alpha\Delta(T)$, where α is a dimensionless parameter measuring the effective mode gap, e.g., $\alpha \sim 1$ for MgB₂. The quality factor $Q \equiv \omega_{L,0}\tau_D/2$, where τ_D is the mode damping time. We note that the model in Eq. (4) is valid in the semiclassical regime $\hbar\omega_{L,0}/k_B \ll T < T_c$, where energy level quantization can be neglected. Equation (4) can be solved readily. For low quality factors $Q < 1/2$, only overdamped solutions exist. For high quality factors $Q \geq 1/2$, the underdamped solutions are present, $\phi(t) \propto e^{-t/\tau_D} \cos(\omega_L t + \theta)$, where $\omega_L^2 = \omega_{L,0}^2 - \tau_D^{-2}$ and θ depend on the initial condition. The underdamped mode leads to the oscillatory reflectivity changes

$$(\Delta R/R)_L = -\mathcal{B}e^{-t/\tau_D} \cos(\omega_L t + \theta), \quad (5)$$

where \mathcal{B} is proportional to the initial phase amplitude, and $\omega_L = 2\pi\nu_L$ with ν_L being the linear frequency manifested in reflectivity signals.

Figure 3(a) shows the subnanosecond transient reflectivity changes $\Delta R/R$ as functions of pump fluence at $T = 5, 20, 30$, and 50 K, and Fig. 3(b) shows the oscillatory components $(\Delta R/R)_L$ at $T = 5, 20$ K. The fast Fourier transform (FFT) analysis of $T = 20$ K signals is presented in Figs. 3(c) and 3(d). Figure 4(a) shows $(\Delta R/R)_L$ as functions of temperature for $F = 120$ and $180 \mu\text{J}/\text{cm}^2$. We fit $F = 120 \mu\text{J}/\text{cm}^2$ signals by using Eq. (5) and depict the temperature dependence of the mode characteristic parameters in Figs. 4(b)–4(d). In correspondence, we summarize the zero-temperature parameters in Table I.

We identify the coherent oscillations as a soft Leggett mode. The oscillations exhibit a single frequency $\nu_L \approx 5$ GHz for $T < T_v \approx 29$ K $< T_c$, that is almost fluence- and temperature-independent below T_v [Figs. 3(c) and 4(c)], and the energy $\hbar\omega_{L,0} \approx 21 \mu\text{eV}$ is negligibly low with $\alpha \sim 10^{-3}$. Moreover, the oscillations suddenly become invisible at T_v before the SC transition occurs [Fig. 4(b)]. Evidently, the oscillations reflect a soft collective mode associated with the superconductivity. We rule out the hard modes, such as the Bogoliubov-Anderson-Goldstone mode [52] and the Higgs mode [53], and the Bardasis-Schrieffer mode due to the proximity of s - and d -wave channels [54]. The discrepancy between T_v and T_c can originate from various factors. For example, the oscillation period may rapidly exceed the measurement time domain as the SC gaps close. On the other hand, thermal noises could diminish the mode as temperature increases. We notice a very similar discrepancy in MgB₂

($T_c \approx 38$ K), in which the measured Leggett mode is completely damped above 26 K [19]. We confirm that the model in Eq. (4) is valid for our experiment since $T \gg \hbar\omega_{L,0}/k_B \approx 0.3$ K.

The damping time τ_D increases with temperature and shows a tendency of divergence close to T_c [Fig. 4(c)]. This tendency suggests that the mode damping might be related to the SC gaps or the QP decay governed by the boson-bottleneck effect. We estimate the initial phase of the mode $\theta = -0.8 \pm 0.1 \approx -\pi/4$, which is almost temperature- and fluence-independent below T_v . At a fixed temperature below T_v , the 5 GHz intensity is almost linear in F for low fluence and gets saturated for high fluence [Fig. 3(d)]. This indicates that the Raman stimulation contribution to the mode generation dominates in low fluence regime and unwanted thermal effects like joule heating possibly become non-negligible in the high fluence regime. For a fixed fluence, \mathcal{B} significantly decreases close to T_v [Fig. 4(d)].

We note that the Leggett mode in CaKFe₄As₄ with $\alpha \sim 10^{-3}$ is dramatically softened compared to the one in MgB₂ with $\alpha \sim 1$ [5,15–19]. The presence of this soft Leggett mode conflicts with the two-band theory for pnictides [13], but agrees with the theory of the spontaneous time-reversal-symmetry breaking state in three- or four-band superconductors [11–14]. A microscopic derivation of the Leggett mode in CaKFe₄As₄ seems tedious, since the number of the SC gaps is not clear and the pair couplings are complicated [27]. However, it is evident that there exist more than four bands and the competition between various pairing channels is significant. Therefore, interband phase frustration ought to be unexceptional and lead to a massless Leggett mode at the mean-field level. In experiment, a small mass can be observed due to weak energy dispersion or quantum fluctuation corrections [14]. This is presumably the origin of the 5 GHz oscillations in our work. In principle, the measured frequency is closely determined by mode dispersion/velocity and conductivity/refractive index, similar to the signals of coherent acoustic phonons [37,55]. These parameters are hardly gained from the present works, and we leave the microscopic calculation to future study. In addition, to clarify the damping mechanisms and the temperature and fluence dependence of the photoexcited amplitude and phase, further measurements are essentially required.

IV. CONCLUSION

In summary, in SC CaKFe₄As₄ we observed a long-lived low-frequency oscillation by time-resolved optical reflectivity technique. We argue that this oscillation corresponds to the soft Leggett mode that indicates the time-reversal-symmetry breaking state in the unconventional s -wave superconductors. Our finding also indicates that the time-resolved technique is a powerful tool for investigating peculiar low-energy collective modes in strongly correlated systems.

ACKNOWLEDGMENTS

The authors gratefully acknowledge support from the National Natural Science Foundation of China (Grants No.

51875006 and No. 51705009), and the Key Project of Beijing Municipal Natural Science Foundation and Beijing Educa-

tion Committees Science and Technology Plan (Grant No. KZ201810005001).

- [1] A. J. Leggett, *Prog. Theor. Phys.* **36**, 901 (1966); *Rev. Mod. Phys.* **47**, 331 (1975).
- [2] A. V. Balatsky, P. Kumar, and J. R. Schrieffer, *Phys. Rev. Lett.* **84**, 4445 (2000).
- [3] S. Maiti and P. J. Hirschfeld, *Phys. Rev. B* **92**, 094506 (2015).
- [4] N. Bittner, D. Einzel, L. Klam, and D. Manske, *Phys. Rev. Lett.* **115**, 227002 (2015).
- [5] S. C. Sharapov, V. P. Gusynin, and H. Beck, *Eur. Phys. J. B* **30**, 45 (2002).
- [6] F. J. Burnell, J. Hu, M. M. Parish, and B. A. Bernevig, *Phys. Rev. B* **82**, 144506 (2010).
- [7] T. Cea and L. Benfatto, *Phys. Rev. B* **94**, 064512 (2016).
- [8] W. Huang, M. Sigrist, and Z.-Y. Weng, *Phys. Rev. B* **97**, 144507 (2018).
- [9] Y. Ota, M. Machida, T. Koyama, and H. Aoki, *Phys. Rev. B* **83**, 060507(R) (2011).
- [10] W. Huang, T. Scaffidi, M. Sigrist, and C. Kallin, *Phys. Rev. B* **94**, 064508 (2016).
- [11] J. Carlström, J. Garaud, and E. Babaev, *Phys. Rev. B* **84**, 134518 (2011).
- [12] S.-Z. Lin and X. Hu, *Phys. Rev. Lett.* **108**, 177005 (2012).
- [13] M. Marciani, L. Fanfarillo, C. Castellani, and L. Benfatto, *Phys. Rev. B* **88**, 214508 (2013).
- [14] K. Kobayashi, M. Machida, Y. Ota, and F. Nori, *Phys. Rev. B* **88**, 224516 (2013).
- [15] Y. G. Ponomarev, S. A. Kuzmicheva, M. G. Mikheev, M. V. Sudakova, S. N. Tchesnokov, N. Z. Timergaleev, A. Yarigin, E. G. Maksimov, S. I. Krasnosvobodtsev, A. Varlashkin, M. A. Hein, G. Muller, H. Piel, L. G. Sevastyanova, O. Kravchenko, K. P. Burdina, and B. M. Bulychev, *Solid State Commun.* **129**, 85 (2004).
- [16] A. Brinkman, S. H. W. van der Ploeg, A. A. Golubov, H. Rogalla, T. H. Kim, and J. S. Moodera, *J. Phys. Chem. Solids* **67**, 407 (2006).
- [17] G. Blumberg, A. Mialitsin, B. S. Dennis, M. V. Klein, N. D. Zhigadlo, and J. Karpinski, *Phys. Rev. Lett.* **99**, 227002 (2007).
- [18] D. Mou, R. Jiang, V. Taufour, R. Flint, S. L. Bud'ko, P. C. Canfield, J. S. Wen, Z. J. Xu, G. Gu, and A. Kaminski, *Phys. Rev. B* **91**, 140502(R) (2015).
- [19] F. Giorgianni, T. Cea, C. Vicario, C. P. Hauri, W. K. Withanage, X. Xi, and L. Benfatto, *Nat. Phys.* **15**, 341 (2019).
- [20] J. Paglione and R. L. Greene, *Nat. Phys.* **6**, 645 (2010).
- [21] A. Chubukov, *Annu. Rev. Condens. Matter Phys.* **3**, 57 (2012).
- [22] For a review of $AeAFe_4As_4$ ($Ae = Ca, Sr, Eu$, and $A = K, Rb, Cs$) compounds, see A. Iyo, K. Kawashima, T. Kinjo, T. Nishio, S. Ishida, H. Fujihisa, Y. Gotoh, K. Kihou, H. Eisaki, and Y. Yoshida, *J. Amer. Chem. Soc.* **138**, 3410 (2016); W. R. Meier, T. Kong, S. L. Bud'ko, and P. C. Canfield, *Phys. Rev. Mater.* **1**, 013401 (2017).
- [23] D. X. Mou, T. Kong, W. R. Meier, F. Lochner, L. L. Wang, Q. S. Lin, Y. Wu, S. L. Bud'ko, I. Eremin, D. D. Johnson, P. C. Canfield, and A. Kaminski, *Phys. Rev. Lett.* **117**, 277001 (2016).
- [24] W. R. Meier, T. Kong, U. S. Kaluarachchi, V. Taufour, N. H. Jo, G. Drachuck, A. E. Böhmer, S. M. Saunders, A. Sapkota, A. Kreyssig, M. A. Tanatar, R. Prozorov, A. I. Goldman, F. F. Balakirev, A. Gurevich, S. L. Bud'ko, and P. C. Canfield, *Phys. Rev. B* **94**, 064501 (2016).
- [25] R. Yang, Y. Dai, B. Xu, W. Zhang, Z. Qiu, Q. Sui, C. C. Homes, and X. Qiu, *Phys. Rev. B* **95**, 064506 (2017).
- [26] T. Xie, Y. Wei, D. L. Gong, T. Fennell, U. Stuhr, R. Kajimoto, K. Ikeuchi, S. L. Li, J. P. Hu, and H. Q. Luo, *Phys. Rev. Lett.* **120**, 267003 (2018).
- [27] F. Lochner, F. Ahn, T. Hickel, and I. Eremin, *Phys. Rev. B* **96**, 094521 (2017).
- [28] J. Cui, Q.-P. Ding, W. R. Meier, A. E. Böhmer, T. Kong, V. Borisov, Y. Lee, S. L. Bud'ko, R. Valentí, P. C. Canfield, and Y. Furukawa, *Phys. Rev. B* **96**, 104512 (2017).
- [29] W.-L. Zhang, W. R. Meier, T. Kong, P. C. Canfield, and G. Blumberg, *Phys. Rev. B* **98**, 140501(R) (2018).
- [30] M. V. Klein, *Phys. Rev. B* **82**, 014507 (2010).
- [31] H. Krull, N. Bittner, G. S. Uhrig, D. Manske, and A. P. Schnyder, *Nat. Commun.* **7**, 11921 (2016).
- [32] Y. Murotani, N. Tsuji, and H. Aoki, *Phys. Rev. B* **95**, 104503 (2017).
- [33] E. E. M. Chia, J. X. Zhu, D. Talbayev, and A. J. Taylor, *Phys. Status Solidi RRL* **5**, 1 (2011).
- [34] J. Demsar, K. Biljaković, and D. Mihailovic, *Phys. Rev. Lett.* **83**, 800 (1999).
- [35] D. H. Torchinsky, F. Mahmood, A. T. Bollinger, I. Božović, and N. Gedik, *Nat. Mater.* **12**, 387 (2013).
- [36] A. V. Bragas, C. Aku-Leh, S. Costantino, Alka Ingale, J. Zhao, and R. Merlin, *Phys. Rev. B* **69**, 205306 (2004).
- [37] S. Kumar, L. Harnagea, S. Wurmehl, B. Buchner, and A. K. Sood, *Euro. Phys. Lett.* **100**, 57007 (2012).
- [38] J. Zhao, A. V. Bragas, D. J. Lockwood, and R. Merlin, *Phys. Rev. Lett.* **93**, 107203 (2004).
- [39] R. Matsunaga, N. Tsuji, H. Fujita, A. Sugioka, K. Makise, Y. Uzawa, H. Terai, Z. Wang, H. Aoki, and R. Shimano, *Science* **345**, 1145 (2014).
- [40] J. Demsar, R. Hudej, J. Karpinski, V. V. Kabanov, and D. Mihailovic, *Phys. Rev. B* **63**, 054519 (2001).
- [41] J. Demsar, R. D. Averitt, A. J. Taylor, V. V. Kabanov, W. N. Kang, H. J. Kim, E. M. Choi, and S. I. Lee, *Phys. Rev. Lett.* **91**, 267002 (2003).
- [42] Y. H. Liu, Y. Toda, K. Shimatake, N. Momono, M. Oda, and M. Ido, *Phys. Rev. Lett.* **101**, 137003 (2008).
- [43] X. C. Nie, H. Y. Song, X. Zhang, Y. Wang, Q. Gao, L. Zhao, X. J. Zhou, J. Q. Meng, Y. X. Duan, H. Y. Liu, and S. B. Liu, *Physica C: Superconductivity and its applications* **577**, 1353710 (2020).
- [44] D. H. Torchinsky, G. F. Chen, J. L. Luo, N. L. Wang, and N. Gedik, *Phys. Rev. Lett.* **105**, 027005 (2010).
- [45] D. H. Torchinsky, J. W. McIver, D. Hsieh, G. F. Chen, J. L. Luo, N. L. Wang, and N. Gedik, *Phys. Rev. B* **84**, 104518 (2011).

- [46] E. E. M. Chia, D. Talbayev, J. X. Zhu, H. Q. Yuan, T. Park, J. D. Thompson, C. Panagopoulos, G. F. Chen, J. L. Luo, N. L. Wang, and A. J. Taylor, *Phys. Rev. Lett.* **104**, 027003 (2010).
- [47] D. Mihailovic, *Phys. Rev. Lett.* **94**, 207001 (2005).
- [48] C. Giannetti, M. Capone, D. Fausti, M. Fabrizio, F. Parmigiani, and D. Mihailovic, *Adv. Phys.* **65**, 58 (2016).
- [49] I. M. Vishik, F. Mahmood, Z. Alpichshev, N. Gedik, J. Higgins, and R. L. Greene, *Phys. Rev. B* **95**, 115125 (2017).
- [50] A. Rothwarf and B. N. Taylor, *Phys. Rev. Lett.* **19**, 27 (1967).
- [51] V. V. Kabanov, J. Demsar, B. Podobnik, and D. Mihailovic, *Phys. Rev. B* **59**, 1497 (1999).
- [52] N. N. Bogoliubov, V. V. Tolmatshev, and D. V. Shirkov, *New Method in the Theory of Superconductivity* (Publisher Consultants Bureau, New York, 1959); P. W. Anderson, *Phys. Rev.* **112**, 1900 (1958).
- [53] For a review, see D. Pekker and C. Varma, *Annu. Rev. Condens. Matter Phys.* **6**, 269 (2015).
- [54] A. Bardasis and J. R. Schrieffer, *Phys. Rev.* **121**, 1050 (1961).
- [55] C. Thomsen, H. T. Grahn, H. J. Maris, and J. Tauc, *Phys. Rev. B* **34**, 4129 (1986).